# Adsorption Properties of Activated Carbons Prepared from Waste CDs and DVDs

Jerzy Choma,[†] Michal Marszewski,[‡] Lukasz Osuchowski,[§] Jacek Jagiello,[⊥] Aleksandra Dziura,[†] and Mietek Jaroniec*,[‡]

[†]Institute of Chemistry, Military Technical Academy, 00-908 Warsaw, Poland

[‡]Department of Chemistry and Biochemistry, Kent State University, Kent, Ohio 44242, United States

[§]Military Institute of Chemistry and Radiometry, 00-910 Warsaw, Poland

[⊥]Micromeritics Instrument Corp., Norcross, Georgia 30093, United States

ABSTRACT: Two sets of activated carbons have been prepared from waste CDs and DVDs by carbonization and subsequent activation with either KOH or CO_2. The resulting activated carbons had specific surface area in the range of 500–2240 m^2 g^{-1}, total pore volume in the range of 0.18–1.36 cm^3 g^{-1}, volume of micropores and small mesopores ($w < \sim 2.9$ nm) in the range of 0.17–1.25 cm^3 g^{-1}, and volume of small micropores ($w < \sim 1.2$ nm) in the range of 0.14–0.71 cm^3 g^{-1}. Both KOH and CO_2 activation resulted in 5–45-fold improvement in the structural properties, depending on the conditions used. The resulting carbons showed good adsorption properties toward carbon dioxide, hydrogen, and benzene. The best uptakes for these adsorptives were 5.8 mmol g^{-1} of CO_2 at 0 °C and 800 mmHg, 3.3 mmol g^{-1} of CO_2 at 25 °C and 850 mmHg, 13.9 mmol g^{-1} of H_2 at −196 °C and 850 mmHg, and 15.4 mmol g^{-1} of C_6H_6 at 20 °C and saturation pressure. The excellent adsorption properties of the prepared carbons render them as potential adsorbents in CO_2 capture and storage, VOCs adsorption/separation, and hydrogen storage.

KEYWORDS: Waste optical discs, KOH activation, CO_2 activation, CO_2 adsorption, hydrogen adsorption, benzene adsorption
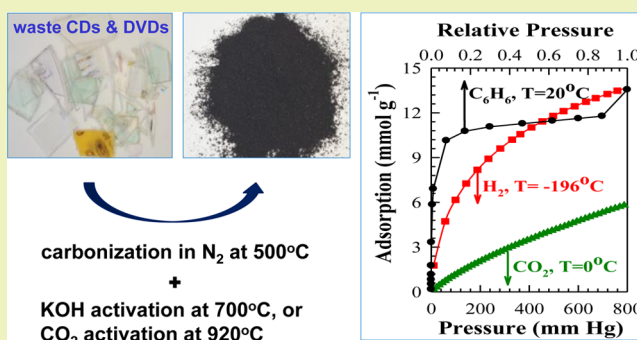
INTRODUCTION

Activated carbons are most commonly prepared from natural precursors such as coal, lignite, peat, wood, and seeds.[1−4] In addition, synthetic wastes may be used as carbon precursors as well. Especially ubiquitous polymers, polyethylene (PE), polypropylene (PP), polystyrene (PS), poly(vinyl chloride) (PVC), poly(ethylene terephthalate) (PET), poly(methyl methacrylate) (PMMA), polyacrylonitrile (PAN), etc., are valuable carbon sources.[5−9] These and many more are used in the production of numerous disposable everyday items, construction elements, cloths, hardware, etc. Although not every polymer is a good carbon precursor, most of the available polymeric wastes can be used to prepare activated carbons.

Laszlo et al.[10] prepared activated carbons from waste PAN and PET by carbonization in nitrogen at 700 °C and subsequent activation with water vapor at 900 °C. Specific surface area of the resulting carbons was 544 m^2 g^{-1} for the PAN precursor and 1254 m^2 g^{-1} for the PET precursor. Bratek et al.[11] prepared activated carbons from a commercial ion-exchange resin Amberjet 1200H used in water treatment. The resin was carbonized at 600 °C and activated with CO_2 at 850 °C, resulting in an activated carbon having specific surface area of 500 m^2 g^{-1}. Choma et al.[12] prepared activated carbons from the same resin, but used KOH for its activation instead of CO_2.

The resulting carbons had markedly higher values of the structural parameters, with the specific surface area reaching 3870 m^2 g^{-1} and total pore volume reaching 2.07 cm^3 g^{-1}. Thanks to extremely well-developed structure, these carbons achieved very good sorption properties toward CO_2 and H_2.

PET is another popular polymeric carbon precursor.[13−15] Kartel et al.[13] prepared porous carbons from PET bottles by impregnation of the shredded bottles with sulfuric acid and thermal treatment at 500−800 °C. The resulting carbons had specific surface area in the range 600−1000 m^2 g^{-1} and total pore volume in the range 0.3−0.8 cm^3 g^{-1}. Esfandiari et al.[14] prepared an activated carbon by carbonization of waste PET and subsequent activation with CO_2. The resulting carbon showed specific surface area of ca. 800 m^2 g^{-1} and iodine value of ca. 630 mg I_2 g^{-1}. Similarly, Bratek et al.[15] prepared activated carbons from waste PET by carbonization in nitrogen and activation with CO_2. Interestingly, in this case, the best material showed specific surface area of 1830 m^2 g^{-1} and total pore volume of 0.7 cm^3 g^{-1}. The authors proposed to use the resulting materials as electrodes in supercapacitors and fuel

cells. Finally, Czepirski et al.[16] investigated porous structures of activated carbons prepared from different waste polymers: PET, PMMA, and phenol-formaldehyde resin. The polymers were first carbonized and subsequently activated using H_2O, CO_2, or KOH. The most developed structure was achieved for KOH-activated carbon prepared from phenol-formaldehyde resin, achieving specific surface area of 3300 m^2 g^{-1} and total pore volume of 1.75 cm^3 g^{-1}. For more examples of activated carbons prepared from various precursors, including waste materials, see the review paper by Dias et al.[17] and references therein. However, details about chemistry of carbonization process can be found in the review paper by Libra et al.[18]

In this work, we prepared two sets of activated carbons by carbonization of waste CDs and DVDs and subsequent activation with either KOH or CO_2. Optical discs are produced from polycarbonates covered with thin layers of organic dye, metal, and lacquer. Polycarbonates are amorphous, thermoplastic polymers produced from bisphenol A, a compound containing two benzene rings in its structure. The latter gives a good prognosis on the polymer's susceptibility toward carbonization and activation. The resulting activated carbons have been investigated toward adsorption of carbon dioxide, hydrogen, and benzene.

■ EXPERIMENTAL SECTION

Materials. Two sets of activated carbons were prepared by carbonization of waste CDs and DVDs and subsequent activation with either KOH or CO_2.

The exact procedure was as follows: first, ca. 5 g of disc fragments (3−5 mm in size) were treated with 10 wt % HCl (POCh, Poland) in an ultrasonic bath for 45 min and subsequently, washed with distilled water. Then, the fragments were placed in a quartz crucible and carbonized at 500 °C for 1 h in a nitrogen stream (1.8 dm^3 min^{-1}, Messer, Poland) in a muffle furnace. Afterward, the resulting carbon was activated with either KOH (POCh, Poland) or CO_2 (Messer, Poland).

The KOH activation was done by using 1:1, 2:1, 3:1, 4:1, 5:1, and 6:1 KOH:C weight ratios in a nickel crucible at 700 °C for 1 h in flowing nitrogen (1.8 dm^3 min^{-1}) in a muffle furnace. After the activation, the materials were washed with deionized water in a fritted funnel, treated with 10 wt % HCl in an ultrasonic bath for 30 min, and again washed with deionized water in an ultrasonic bath for 45 min. Finally, the washed carbons were dried at 100 °C for 8 h in an oven.

The CO_2 activation was carried out in a muffle furnace using the following procedure: the carbon was heated in flowing nitrogen (1.8 dm^3 min^{-1}) using 5 °C min^{-1} temperature ramp until 920 °C. Then, the flow was switched from nitrogen to CO_2 (25 mL min^{-1}) and the activation was carried for either 1, 3, 5, or 8 h. Afterward, the flow was switched back to nitrogen and the sample was allowed to cool down. The resulting carbon was labeled C. The KOH-activated carbons were labeled C-KOH-x, where x designates the KOH:C weight ratio. The CO_2-activated carbons were labeled C-CO_2-y, where y designates the CO_2 activation time in hours.

Measurements. Nitrogen at −196 °C, carbon dioxide at 0 and 25 °C, and hydrogen at −196 °C adsorption data were collected using a volumetric adsorption analyzer ASAP 2020 manufactured by Micromeritics Instrument Corp. (Norcross, GA, USA). Benzene adsorption at 20 °C was measured using McBain−Bakr gravimetric method on a home-made apparatus equipped with a quartz-spring balance. Each sample was degassed in a vacuum at 200 °C for 2 h prior to every adsorption experiment.

Scanning electron microscopy (SEM) and energy-dispersive X-ray spectroscopy (EDX) data were taken on an Ultra Plus scanning electron microscope manufactured by Zeiss (Germany) equipped with a Quantax 400 EDX detector manufactured by Bruker (Germany) using 2 kV acceleration voltage.

Optical images were taken using a 500D photo camera manufactured by Canon (Japan).

Calculations. Specific surface area (S_{BET}) was calculated from low-temperature nitrogen adsorption data in a relative pressure range of 0.05−0.2 using the Brunauer−Emmett−Teller (BET) method and a nitrogen cross section area of 0.162 nm^2.[19] Total pore volume (V_t) was calculated by conversion of the adsorbed amount of nitrogen at a relative pressure ca. 0.99 to the volume of liquid nitrogen at an experiment temperature.[20] Pore size distribution (PSD) and specific surface area (S_{DFT}) were calculated from low-temperature nitrogen adsorption data using 2D-NLDFT method for carbons with slit-shaped pores by taking into account the energetic heterogeneity and geometrical corrugation of the surface[21,22] (the SAIEUS software developed by Jagiello). The volume of small micropores (V_1) was calculated by integration of PSD under the first peak in the range up to w_{r1}, where w_{r1} is the PSD minimum after the first peak. The volume of micropores and small mesopores (V_2) was calculated by integration of PSD under the first and second peak in the range up to w_{r2}, where w_{r2} was chosen as the endpoint of the second peak. Microporosity was calculated as the ratio of V_2 to V_t and expressed in %.

■ RESULTS AND DISCUSSION

The goal of this work was to use waste CDs and DVDs as carbon precursors and prepare activated carbons with well-developed structural properties. The resulting activated carbons were intended as adsorbents in environmental and energy-related applications including CO_2 capture and storage, H_2 storage, and VOC adsorption.

Morphology and Elemental Analysis. Figure 1 shows photographs of the disc fragments, C carbon, and C-KOH-4

Figure 1. Photographs of disc fragments (A), C carbon (B), and C-KOH-4 (C), and C-CO_2-8 (D) activated carbons.

and C-CO_2-8 activated carbons. Morphology of three carbons is different, with C-KOH-4 having the smallest particles, C-CO_2-8 having intermediate-sized grains and C having the biggest grains.

In addition, the sizes of C and C-CO_2-8 particles are similar because CO_2 activation does not change the morphology much, whereas the particles of C-KOH-4 are much smaller because the KOH activation often disintegrates the agglomerated carbon particles and, depending on the initial carbonization

temperature and activation conditions, can partially or completely destroy mesoporous structure.

Figure 2 shows a scanning electron microscopy (SEM) image of the C-KOH-4 carbon, and Table 1 provides the elemental
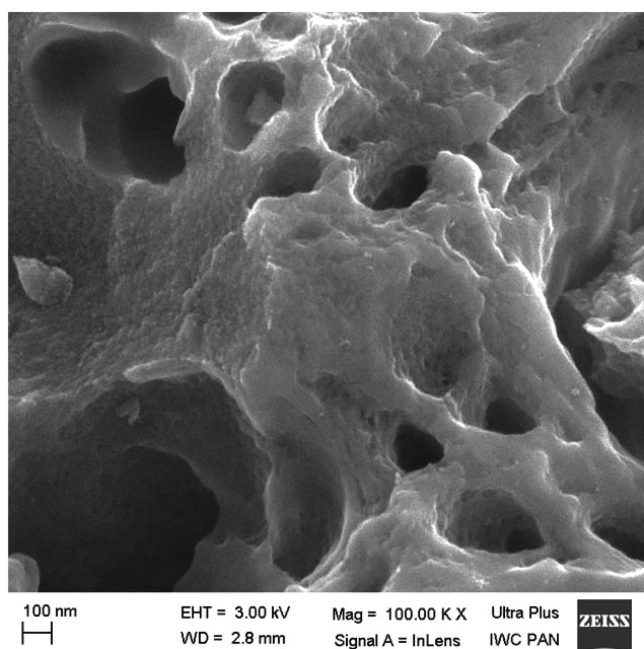

Figure 2. Scanning electron micrograph of the C-KOH-4-activated carbon.

Table 1. Elemental Composition of the Selected KOH-Activated Carbons Prepared from Waste CDs and DVDs

	elemental composition (wt %)[a]			
sample	carbon	oxygen	nitrogen	chlorine
C-KOH-4	84.8	7.9	7.3	
C-KOH-5	87.1	5.9	7.0	0.1
C-KOH-6	86.5	6.7	6.7	0.1

[a]weight content of the listed elements established using an energy-dispersive X-ray spectrometer Quantax 400 manufactured by Bruker (Germany) installed on a scanning electron microscopy Ultra Plus instrument manufactured by Zeiss (Germany).

composition of the selected KOH-activated carbons obtained by energy-dispersive X-ray spectroscopy (EDX). Based on the SEM image, the material shows clearly an irregular macro-porosity (pores above 50 nm), most probably after the KOH activation. In addition, except for carbon (86 wt % on the average), the materials contain oxygen (~6.8 wt %), nitrogen (~7.0 wt %), and trace amounts of chlorine (up to 0.1 wt %, most probably from the HCl used during preparation).

Nitrogen Adsorption Characterization of the Carbons Studied. Figures 3 and 4 show low-temperature nitrogen adsorption−desorption isotherms and Table 2 lists structural parameters calculated based on the nitrogen data for all carbon materials. All isotherms are of Type I according to the IUPAC classification,[23] indicating highly microporous nature of the carbons studied. In the case of KOH-activated carbons, the specific surface area (S_{DFT}) varies from 920 to 2240 $m^2 g^{-1}$, the apparent BET specific surface area (S_{BET}) varies from 730 to 2710 $m^2 g^{-1}$, the total pore volume (V_t) varies from 0.35 to
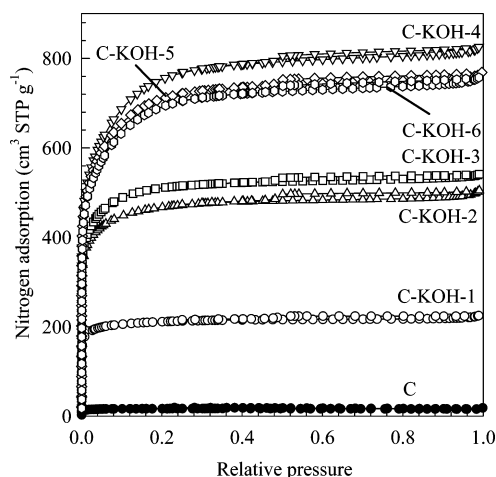

Figure 3. Nitrogen adsorption−desorption isotherms measured at −196 °C for the KOH-activated carbons prepared from waste CDs and DVDs.
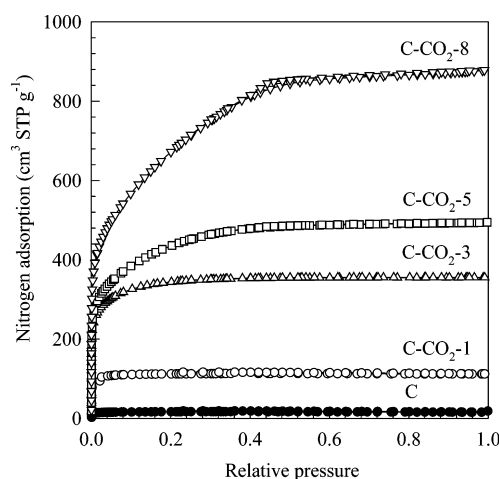

Figure 4. Nitrogen adsorption−desorption isotherms measured at −196 °C for the CO_2-activated carbons prepared from waste CDs and DVDs.

1.27 $cm^3 g^{-1}$, and the volume of micropores and small mesopores (V_2) varies from 0.32 to 1.15 $cm^3 g^{-1}$. All these parameters initially increase with the KOH:C ratio, achieving maximum for the C-KOH-4-activated carbon, and decrease thenceforth. For the CO_2-activated carbons, S_{DFT} varies from 500 to 1840 $m^2 g^{-1}$, S_{BET} varies from 390 to 2440 $m^2 g^{-1}$, V_t varies from 0.18 to 1.36 $cm^3 g^{-1}$, and V_2 varies from 0.17 to 1.25 $cm^3 g^{-1}$. In this case, all structural parameters increase throughout the series, along with the activation time, and the highest values are for the C-CO_2-8-activated carbon. The C material did not show well-developed structure with S_{DFT} of 100 $m^2 g^{-1}$, S_{BET} of 66 $m^2 g^{-1}$, and V_t of 0.03 $cm^3 g^{-1}$.

Figures 5 and 6 show differential pore size distributions (PSD) calculated using NLDFT method based on the nitrogen data. The PSD curves for all carbons exhibit two distinctive peaks, which signify the presence of two pore fractions in these materials: the first fraction of small micropores (mainly ultramicropores and small supermicropores), and the second fraction of large micropores and small mesopores. The pore sizes of these fractions (w_1 and w_2) were estimated from the respective peaks' maxima. In addition, the volume of the small micropores (V_1) and the volume of micropores and small

Table 2. Structural Parameters Calculated on the Basis of Low-Temperate Nitrogen Adsorption Data for All Carbon Materials Prepared from Waste CDs and DVDs[a]

sample	S_{DFT} (m^2 g^{-1})	S_{BET} (m^2 g^{-1})	V_t (cm^3 g^{-1})	V_2 (cm^3 g^{-1})	V_1 (cm^3 g^{-1})	w_1 (nm)	w_2 (nm)	w_{r1} (nm)	w_{r2} (nm)	microporosity (%)
C	100	66	0.03	0.03	0.02	0.5	1.2	1.0	1.8	100
C-KOH-1	920	730	0.35	0.32	0.27	0.6	1.3	1.1	2.6	91
C-KOH-2	1660	1620	0.78	0.70	0.58	0.7	1.6	1.3	2.9	90
C-KOH-3	1830	1800	0.84	0.77	0.57	0.7	1.4	1.2	2.8	92
C-KOH-4	2240	2710	1.27	1.15	0.68	0.8	1.7	1.3	3.1	91
C-KOH-5	2190	2540	1.18	1.07	0.68	0.7	1.7	1.3	2.9	91
C-KOH-6	2000	2480	1.17	1.05	0.71	0.8	1.7	1.4	3.1	90
C-CO$_2$-1	500	390	0.18	0.17	0.14	0.6	1.2	1.0	1.8	94
C-CO$_2$-3	1200	1210	0.55	0.52	0.37	0.7	1.5	1.2	2.6	95
C-CO$_2$-5	1320	1560	0.77	0.71	0.38	0.7	1.9	1.3	3.8	92
C-CO$_2$-8	1840	2440	1.36	1.25	0.48	0.9	2.0	1.4	4.8	92

[a]Notation: S_{DFT}, specific surface area calculated using the 2D-NLDFT method for carbons with slit-shaped pores under assumptions of energetic heterogeneity and geometrical corrugation of the surface implemented in the SAIEUS software; S_{BET}, apparent specific surface area calculated by the Brunauer−Emmett−Teller method using low-temperature nitrogen adsorption data in the relative pressure range of 0.05−0.2 and nitrogen cross section molecular area of 0.162 nm^2; V_v, single-point pore volume calculated by conversion of the nitrogen adsorption at a relative pressure ca. 0.99 to the volume of liquid nitrogen at an experiment temperature; V_2, volume of micropores and small mesopores calculated by integration of PSD under the first and second peak in the range up to w_{r2}, where w_{r2} is defined as the endpoint of the second peak; V_1, volume of small micropores calculated by integration of PSD under the first peak in the range up to w_{r1}, where w_{r1} is defined as the PSD minimum after the first peak; w_1, size of small micropores estimated at the maximum of the first PSD peak; w_2, size of large micropores estimated at the maximum of the second PSD peak; w_{r1}, position of the PSD minimum after the first peak used to calculate V_1; w_{r2}, endpoint of the second peak used to calculate V_2; microporosity, ratio of V_2 to V_t expressed in %.
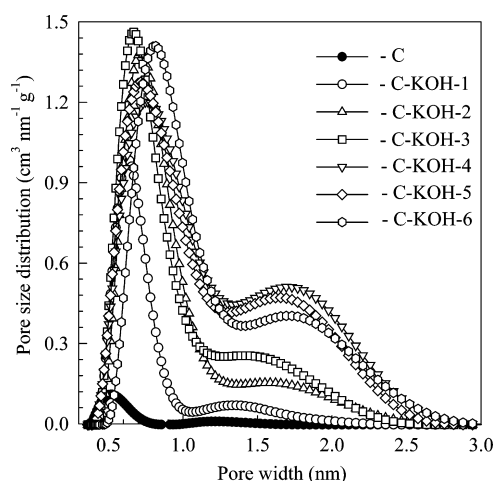
Figure 5. Differential pore size distribution functions for the KOH-activated carbons prepared from waste CDs and DVDs (calculated by the 2D-NLDFT method).
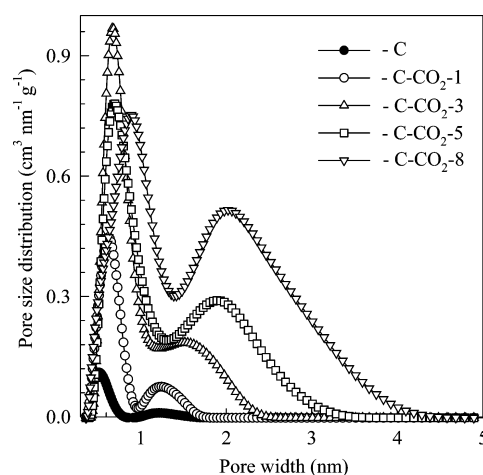
Figure 6. Differential pore size distribution functions for the CO$_2$-activated carbons prepared from waste CDs and DVDs (calculated by the 2D-NLDFT method).

mesopores (V_2) were calculated by integration of the PSD curves under the first and both peaks, respectively. The integration interval varied for different materials due to slightly different peaks' positions and widths. Table 2 lists all these parameters and the integration intervals for all carbon materials. For the KOH-activated materials, small and large micropore sizes change from 0.6 and 1.3 nm for the C-KOH-1 material to 0.8 and 1.7 nm for the C-KOH-6 material, respectively. For the CO$_2$-activated materials, the analogous sizes change from 0.6 and 1.2 nm for the C-CO$_2$-1 material to 0.9 and 2.0 nm for the C-CO$_2$-8 material, respectively. Both micropore sizes somewhat depend on the activation conditions, either the KOH:C ratio or the CO$_2$ purge time. In all instances, these sizes increase with the intensity of the activation; however, a significantly stronger correlation is observed in the case of CO$_2$ activation.

The volume of small micropores varies from 0.27 to 0.71 cm^3 g^{-1} for the KOH-activated carbons and from 0.14 to 0.48 cm^3

g^{-1} for the CO$_2$-activated carbons. In both series, this volume increases with the activation intensity. The volume of micropores and small mesopores varies from 0.32 to 1.15 cm^3 g^{-1} for the KOH-activated carbons and from 0.17 to 1.25 cm^3 g^{-1} for the CO$_2$-activated carbons. In this case, the highest value of this volume is for the C-KOH-4 material, but it increases throughout the series for the CO$_2$-activated carbons.

Microporosity exceeds 90% for all activated carbons, which shows the highly microporous nature of the materials studied. Interestingly, the CO$_2$-activated carbons show slightly higher values as compared to the KOH-activated carbons and a slight decline in the microporosity with activation time.

Properties of the Carbons Studied for CO$_2$ Adsorption. CO$_2$ adsorption measurements are commonly used for characterization of various porous adsorbents, including their potential for CO$_2$ capture.[24−28] Carbon dioxide adsorption was measured for all activated carbons at 0 °C up to 800 mmHg

and at 25 °C up to 850 mmHg. Figures 7−10 show CO_2 adsorption isotherms, and Table 3 lists the maximum CO_2 uptakes for all activated carbons.
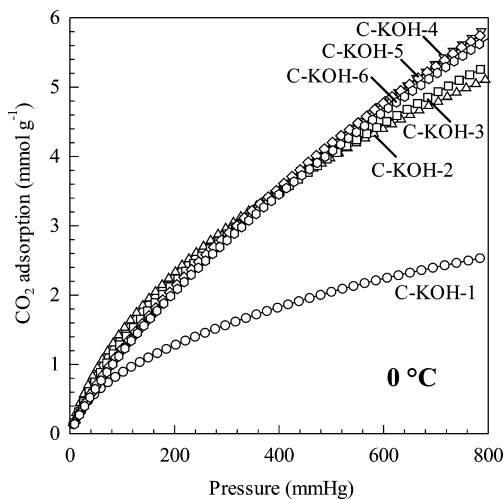

Figure 7. Carbon dioxide adsorption isotherms measured at 0 °C for the KOH-activated carbons prepared from waste CDs and DVDs.
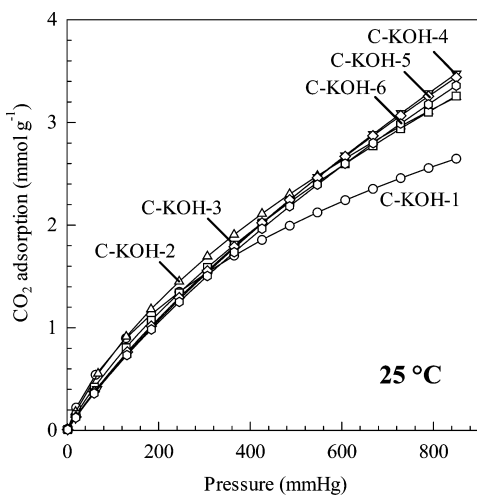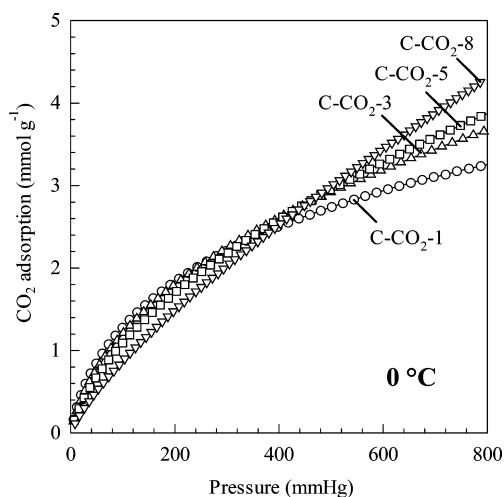

Figure 8. Carbon dioxide adsorption isotherms measured at 25 °C for the KOH-activated carbons prepared from waste CDs and DVDs.

For the KOH-activated carbons, the CO_2 uptake initially increases with the KOH:C ratio, achieving maximum for the C-KOH-4 material, and decreases for the C-KOH-5 and C-KOH-6 carbons. In the case of the CO_2-activated carbons, the CO_2 uptake increases throughout the series, showing the highest value for the C-CO_2-8 material. Conspicuously, the highest CO_2 uptakes, for both KOH- and CO_2-activated carbons, are observed for the materials with the highest values of the structural parameters (S_{DFT}, S_{BET} V_t, V_1, and V_2). Between both series, the C-KOH-4 material scored the highest CO_2 uptakes: 5.8 mmol g^{-1} (0 °C, 800 mmHg) and 3.3 mmol g^{-1} (25 °C, 850 mmHg). In addition, assuming an exponential temperature-dependence of the CO_2 uptake reported by Ludwinowicz and Jaroniec[29] and taking into account the conditions of pressure swing adsorption process[30] (adsorption at 30 °C and 1 atm, desorption at 60 °C and 0.0013 atm), one can estimate the working capacity of the C-KOH-4 sorbent as 2.84 mmol g^{-1} (125 mg g^{-1}), which is a fairly good result.[31]

Figure 9. Carbon dioxide adsorption isotherms measured at 0 °C for the CO_2-activated carbons prepared from waste CDs and DVDs.
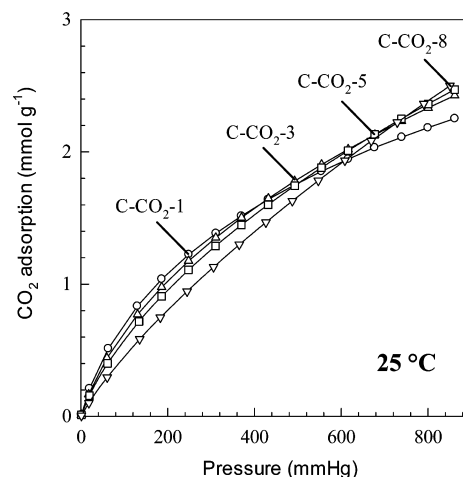

Figure 10. Carbon dioxide adsorption isotherms measured at 25 °C for the CO_2-activated carbons prepared from waste CDs and DVDs.

For the purpose of comparison, Table 3 lists the CO_2, H_2, and C_6H_6 uptakes for two other KOH-activated carbons: C-4 (obtained from styrene divinylbenzene resin with sulfonate functional groups)[12] and KEV-4-KOH (obtained from Kevlar).[32] The gas uptakes of these carbons and the carbons studied differ noticeably; for instance, the Kevlar-derived carbon shows higher C_6H_6 uptake but lower CO_2 uptake as compared to those obtained for best carbons reported in this work, while the C-4 carbon shows both higher CO_2 and H_2 uptakes. The observed difference in the porous structure and surface properties of the carbons listed in Table 3 is an obvious explanation of the different gas uptakes, but the former depend on the carbon precursors used because the conditions of carbonization and activation were almost the same. The gas uptakes listed in Table 3 show the importance of the structure and chemistry of carbon precursors on the adsorption properties of the resulting activated carbons.

Figure 11 shows CO_2 uptakes at 0 °C and 800 mmHg and 25 °C and 850 mmHg as functions of the volume of small micropores (V_1) for the KOH- and CO_2-activated carbons. The straight lines represent linear regressions for two datasets with correlation coefficients $R^2 = 0.889$ for 0 °C and $R^2 = 0.883$ for 25 °C. The high correlation of the two parameters shows that

Table 3. Carbon Dioxide, Hydrogen, and Benzene Uptakes at Indicated Temperatures for All Activated Carbons Prepared from Waste CDs and DVDs[a]

sample	CO_2 uptake (mmol g^{-1})		hydrogen uptake (mmol g^{-1})	benzene uptake (mmol g^{-1})
	0 °C	25 °C	−196 °C	20 °C
C-KOH-1	2.5	2.4	6.8	3.5
C-KOH-2	5.1	3.1	9.8	7.3
C-KOH-3	5.3	3.1	10.5	9.5
C-KOH-4	5.8	3.3	13.9	13.6
C-KOH-5	5.7	3.3	13.1	11.9
C-KOH-6	5.7	3.2	13.0	12.8
C−CO$_2$-1	3.3	2.3	5.7	2.0
C−CO$_2$-3	3.7	2.4	7.3	4.0
C−CO$_2$-5	3.9	2.5	8.3	7.5
C−CO$_2$-8	4.3	2.5	11.3	15.4
C-4[b]	7.8	4.3	18.8	
KEV-4-KOH[c]	4.5	2.7	10.7	17.3

[a]CO_2 uptake, carbon dioxide adsorption at a pressure of ca. 800 mmHg (for 0 °C) or ca. 850 mmHg (for 25 °C); hydrogen uptake, hydrogen adsorption at a pressure of ca. 850 mmHg; benzene uptake, benzene adsorption at a saturation pressure. [b]CO_2 and H_2 uptakes taken from ref 12. [c]CO_2, H_2, and C_6H_6 uptakes taken from ref 32.
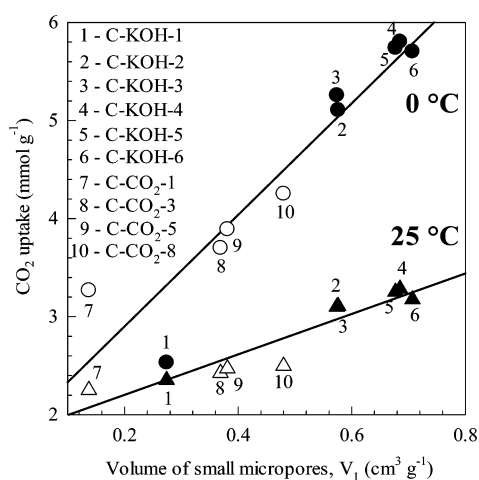

Figure 11. Carbon dioxide uptakes at 0 °C and 800 mmHg (circles) and 25 °C and 850 mmHg (triangles) as functions of the volume of small micropores (V_1) for the KOH-activated (full symbols) and CO_2-activated (hollow symbols) carbons prepared from waste CDs and DVDs.

the CO_2 uptake at these temperatures and pressures is governed by the volume of small micropores, which is in agreement with our previous findings for CO_2 adsorption on activated carbons obtained from a styrene divinylbenzene resin with sulfonate functional groups.[12]

Figure 12 shows the CO_2 uptakes at 0 °C and 800 mmHg and 25 °C and 850 mmHg as functions of the volume of micropores and small mesopores (V_2) for KOH- and CO_2-activated carbons. The straight lines represent linear regressions for two datasets with correlation coefficients $R^2 = 0.595$ for 0 °C and $R^2 = 0.434$ for 25 °C. The much smaller values of the coefficients suggest that the bigger micropores and small mesopores do not determine the CO_2 uptake at these temperatures and pressures.

Finally, Figure 13 shows CO_2 uptakes at 0 °C and 800 mmHg and 25 °C and 850 mmHg as functions of the specific
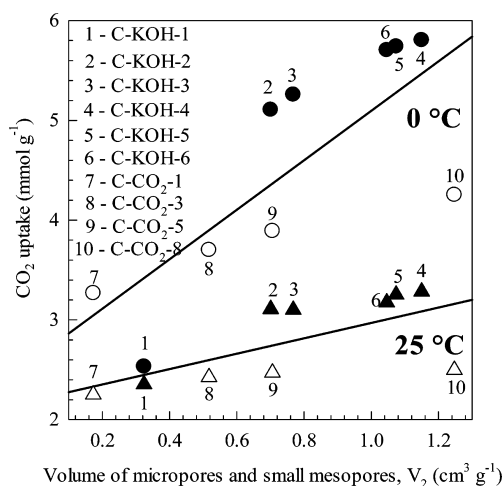

Figure 12. Carbon dioxide uptakes at 0 °C and 800 mmHg (circles) and 25 °C and 850 mmHg (triangles) as functions of the volume of micropores and small mesopores (V_2) for the KOH-activated (full symbols) and CO_2-activated (hollow symbols) carbons prepared from waste CDs and DVDs.
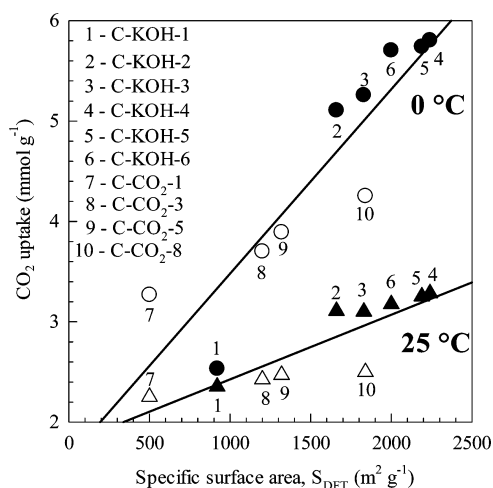

Figure 13. Carbon dioxide uptakes at 0 °C and 800 mmHg (circles) and 25 °C and 850 mmHg (triangles) as functions of the specific surface area (S_{DFT}) for the KOH-activated (full symbols) and CO_2-activated (hollow symbols) carbons prepared from waste CDs and DVDs.

surface area (S_{DFT}) for the KOH- and CO_2-activated carbons. The straight lines represent linear regressions for two datasets with correlation coefficients $R^2 = 0.820$ for 0 °C and $R^2 = 0.758$ for 25 °C. Although the CO_2 uptake shows some correlation with the specific surface area, the fit is not as good as in the case of the volume of small micropores, showing the latter is the structural parameter determining the CO_2 uptake at the ambient temperatures and pressures studied. Consequently, activated carbons intended for CO_2 adsorption should possess possibly large volume of small micropores.

Properties of the Carbons Studied for H_2 Adsorption. Similarly as in the case of CO_2, hydrogen adsorption can be used for characterization of ultramicroporous materials, especially from the viewpoint of their potential for H_2 storage.[33] Hydrogen adsorption was measured for all activated carbons at −196 °C up to 850 mmHg. Figures 14 and 15 show hydrogen isotherms, and Table 3 provides the maximum hydrogen
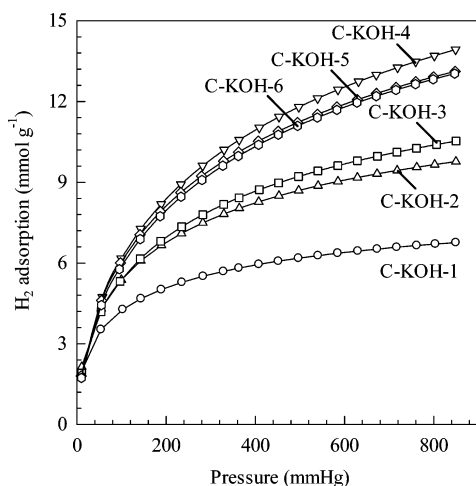
Figure 14. Hydrogen adsorption isotherms measured at −196 °C for the KOH-activated carbons obtained prepared from waste CDs and DVDs.

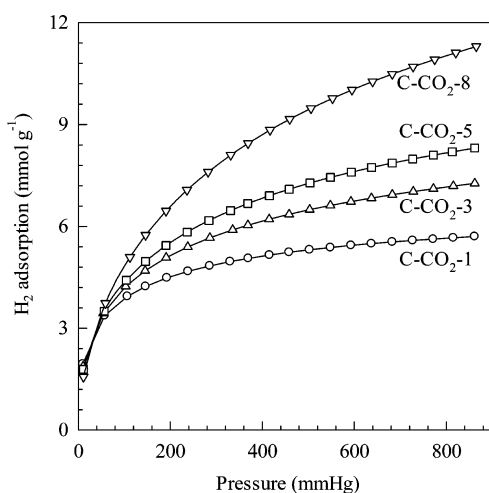**Figure 16.** Hydrogen uptakes at −196 °C and 850 mmHg as a function of the specific surface area (S_{DFT}) for the KOH-activated (full circles) and CO_2-activated carbons (hollow circles) prepared from waste CDs and DVDs.

Figure 15. Hydrogen adsorption isotherms measured at −196 °C for the CO_2-activated carbons prepared from waste CDs and DVDs.

Figure 17. Hydrogen uptakes at −196 °C and 850 mmHg as a function of the volume of small micropores (V_1) for the KOH-activated (full circles) and CO_2-activated carbons (hollow circles) prepared from waste CDs and DVDs.

uptakes for all carbon materials. Similarly to CO_2 adsorption, the hydrogen uptake initially increases with the KOH:C ratio, achieving maximum for the C-KOH-4 carbon, and decreases afterward. For CO_2-activated carbons, the hydrogen uptake increases throughout the series, reaching the highest value for the C-CO$_2$-8 material. The maximum values of adsorbed H$_2$ are 13.9 and 11.3 mmol g^{-1} for the C-KOH-4 and C-CO$_2$-8 materials, respectively.

Figure 16 shows hydrogen uptake at −196 °C and 850 mmHg as a function of the specific surface area (S_{DFT}) for KOH- and CO_2-activated carbons. The straight line is a linear regression with correlation coefficient $R^2 = 0.943$. The high R^2 value indicates that the specific surface area is the structural parameter determining the hydrogen adsorption at this temperature and pressure.

Figure 17 shows hydrogen uptakes at −196 °C and 850 mmHg as a function of the volume of small micropores (V_1) for KOH- and CO_2-activated carbons. The straight line is a linear regression with correlation coefficient $R^2 = 0.897$. Interestingly, the R^2 value for this relation is quite high as well. This indicates that the small micropores play an importnat role in hydrogen adsorption as well; however, it is quite different from the case of
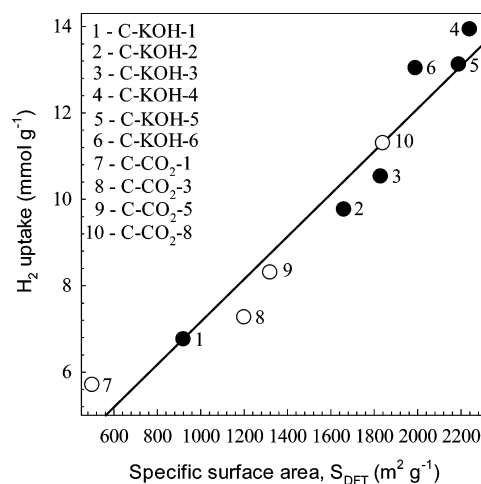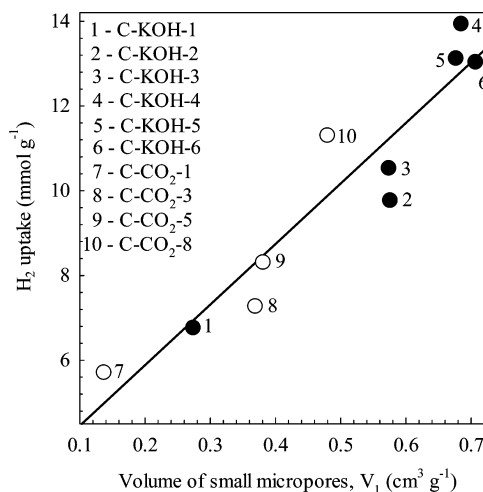
CO_2 adsorption. We postulate that hydrogen, at this temperature and pressure, as a much smaller molecule (as compared to both N$_2$ and CO_2) and well above its boiling point (−252.9 °C), is adsorbed through the film formation rather than volume filling, even in the micropores. The observed correlation with V_1 volume is explained as an indirect correlation to the micropores' surface area (the smallest pores contribute the most to the total surface area) rather than to their volume. Consequently, activated carbons intended for application in hydrogen storage/adsorption should feature the largest possible surface area to achieve the highest hydrogen uptake.

Properties of the Carbons Studied for Benzene Vapor Adsorption. Benzene adsorption at 20 °C was measured on all activated carbons, where benzene was selected as a model volatile organic compound (VOC). Figures 18 and 19 show benzene adsorption isotherms, and Table 3 provides the maximum benzene uptakes for all activated carbons. Benzene adsorption follows the same trend as in the case of CO_2 and H$_2$ adsorption. For the KOH-activated carbons, it increases initially
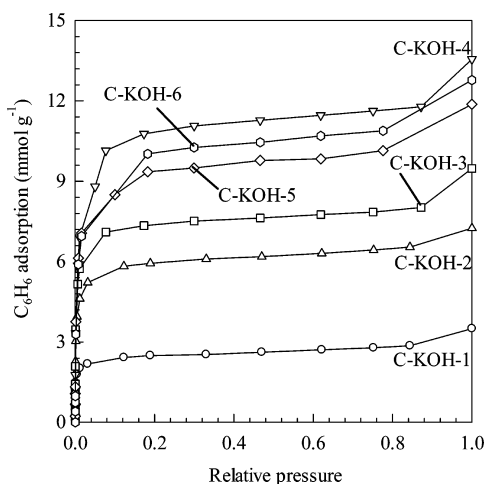
Figure 18. Benzene adsorption isotherms measured at 20 °C for the KOH-activated carbons prepared from waste CDs and DVDs.
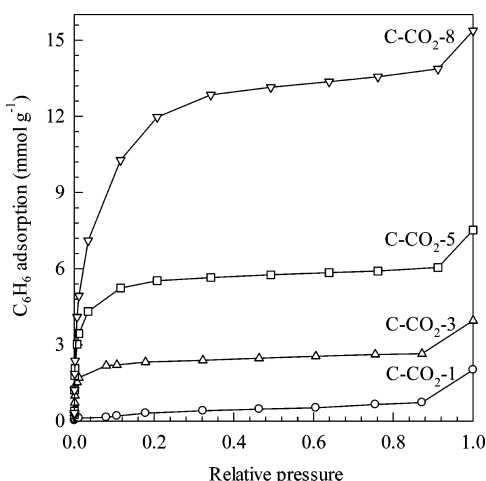

Figure 19. Benzene adsorption isotherms measured at 20 °C for the CO_2-activated carbons prepared from waste CDs and DVDs.

Figure 20. Benzene uptakes at 20 °C and saturation pressure as a function of the volume of micropores and small mesopores (V_2) for the KOH-activated (full circles) and CO_2-activated carbons (hollow circles) prepared from waste CDs and DVDs.

Figure 21. Benzene uptakes at 20 °C and saturation pressure as a function of the specific surface area (S_{DFT}) for the KOH-activated (full circles) and CO_2-activated carbons (hollow circles) prepared from waste CDs and DVDs.

with the KOH:C ratio, achieving maximum for the C-KOH-4 material, and decreases for the C-KOH-5 and C-KOH-6 materials. For the CO_2-activated carbons, the benzene uptake increases throughout the series, showing the highest uptake for the C-CO_2-8 material. The maximum values of adsorbed benzene are 13.6 and 15.4 mmol g^{-1} for the C-KOH-4 and C-CO_2-8 materials, respectively.

Figure 20 shows benzene uptake at 20 °C and saturation pressure as a function of the volume of micropores and small mesopores (V_2) for all activated carbons. The straight line represents linear regression with correlation coefficient R^2 = 0.971. Figure 21 shows the same uptake but as a function of the specific surface area (S_{DFT}). The straight line represents linear regression with correlation coefficient R^2 = 0.811. The high R^2 value for the first relation shows that, for activated carbons and at this temperature and pressure, benzene adsorbs mainly in micropores and small mesopores through the volume filling mechanism rather than the film formation. Consequently, activated carbons intended for benzene and/or VOCs adsorption should possess the largest possible micropore volume to maximize the uptake.
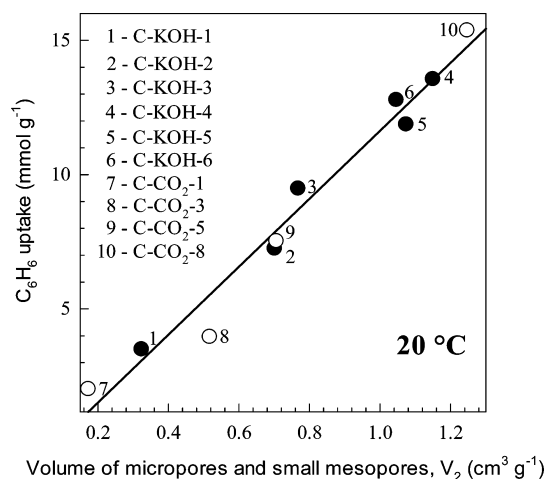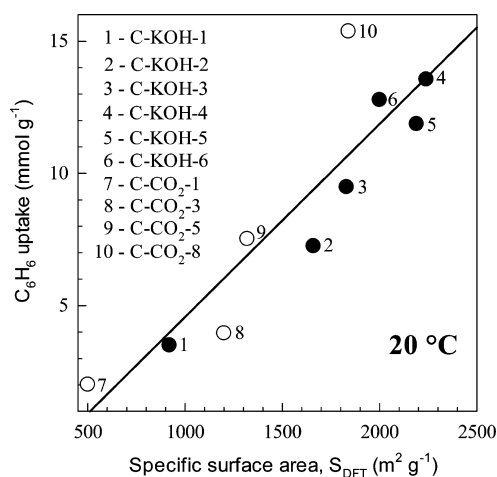
CONCLUSIONS

Two series of activated carbons has been prepared from waste CDs and DVDs by carbonization and subsequent activation with either KOH or CO_2. The resulting carbons featured the well-developed specific surface area (500−2240 m² g^{-1}), large total pore volume (0.18−1.36 cm³ g^{-1}), high volume of micropores and small mesopores (0.17−1.25 cm³ g^{-1}), and high volume of small micropores (0.14−0.71 cm³ g^{-1}).

Both KOH and CO_2 activations are powerful techniques for significant enlargement of the specific surface area and porosity in carbons. As compared to the original carbon, the specific surface area increased 9−22 times after the KOH activation and 5−18 times after the CO_2 activation; the total pore volume increased 12−42 times after the KOH activation and 6−45 times after the CO_2 activation; the volume of micropores and small mesopores increased 11−38 times after the KOH activation and 6−42 times after the CO_2 activation; and the volume of small micropores increased 14−36 times after the KOH activation and 7−24 times after the CO_2 activation.

These high values of the structural parameters resulted in exceptional uptakes of carbon dioxide, hydrogen, and benzene. The highest uptakes for these adsorptives are 5.8 mmol g^{-1} of CO_2 at 0 °C and 800 mmHg, 3.3 mmol g^{-1} of CO_2 at 25 °C and 850 mmHg, 13.9 mmol g^{-1} of H_2 at −196 °C and 850 mmHg, and 15.4 mmol g^{-1} of C_6H_6 at 20 °C and saturation pressure.

Finally, it was established that carbon dioxide and benzene, at the temperatures and pressures studied, adsorb on activated carbons through the micropore filling mechanism. Thus, activated carbons intended for adsorption of CO_2 should possess large volumes of small micropores, and for adsorption of benzene large volume of micropores and small mesopores. In contrast, hydrogen, at the temperature and pressures studied, adsorbs mainly on the surface. Thus, activated carbons intended for hydrogen adsorption/storage should possess large specific surface area.

The excellent adsorption properties of the activated carbons prepared from waste CDs and DVDs render them potential adsorbents in carbon dioxide capture and storage, VOCs adsorption/separation, and hydrogen storage.

■ AUTHOR INFORMATION

Corresponding Author
*Mietek Jaroniec. Fax: +1 (330) 672-3816. Tel: +1 (330) 672-2032. E-mail: jaroniec@kent.edu.

Notes
The authors declare no competing financial interest.

■ ACKNOWLEDGMENTS

■ REFERENCES

(1) Jankowska, H.; Swiatkowski, A.; Choma, J. *Active Carbon*; Ellis Horwood Ltd.: Chichester, U. K., 1991.

(2) Bansal, R. C.; Goyal, M. *Activated Carbon Adsorption*; CRC Press: Boca Raton, FL, 2005.

(3) Marsh, H.; Rodriquez-Reinoso, F. *Activated Carbon*; Elsevier: Amsterdam, 2006.

(4) Bandosz, T. J.; Petit, C. On the reactive adsorption of ammonia on activated carbons modified by impregnation with inorganic compounds. *J. Colloid Interface Sci.* 2009, 338, 329−345.

(5) Mishra, S.; Goje, A. S.; Zope, V. S. Chemical recycling, kinetics, and thermodynamics of poly(ethylene terephthalate) (PET) waste powder by nitric acid hydrolysis. *Polym. React. Eng.* 2003, 11, 79−99.

(6) Arienillas, A.; Rubiera, F.; Parra, J. B.; Ania, C. O.; Pis, J. J. Surface modification of low cost carbons for their application in the environmental protection. *Appl. Surf. Sci.* 2005, 252, 619−624.

(7) Migahead, M. A.; Abdul-Raheim, A. M.; Atta, A. M.; Brostow, W. Synthesis and evaluation of a new water soluble corrosion inhibitor from recycled poly(ethylene terephtalate). *Mater. Chem. Phys.* 2010, 121, 208−214.

(8) Gupta, V. K.; Nayak, A.; Agarwal, S.; Tyagi, I. Potential of activated carbon from waste rubber tire for the adsorption of phenolics: Effect of pre-treatment conditions. *J. Colloid Interface Sci.* 2014, 417, 420−430.

(9) Choma, J.; Osuchowski, L.; Jaroniec, M. Properties and applications of activated carbons obtained from polymeric materials: A review. *Ochr. Srodowiska* 2014, 36, 3−16.

(10) Laszlo, K.; Bota, A.; Nagy, L. G.; Cabasso, I. Porous carbon from polymer waste materials. *Colloids Surf., A* 1999, 151, 311−320.

(11) Bratek, K.; Bratek, W.; Kaluzynski, M. Carbon adsorbents from waste ion-exchange resin. *Carbon* 2002, 40, 2213−2220.

(12) Choma, J.; Osuchowski, L.; Marszewski, M.; Jaroniec, M. Highly microporous polymer-based carbons from CO_2 and H_2 adsorption. *RSC Adv.* 2014, 4, 14795−14802.

(13) Kartel, M. T.; Sych, N. V.; Tsyba, M. M.; Strelko, V. V. Preparation of porous carbons by chemical activation of polyethyleneterephtalate. *Carbon* 2006, 44, 1019−1022.

(14) Esfandiari, A.; Kaghazchi, T.; Soleimani, M. Preparation and evaluation of activated carbons obtained by physical activation of polyethyleneterephtalate (PET) wastes. *J. Taiwan Inst. Chem. Eng.* 2012, 43, 631−637.

(15) Bratek, W.; Swiatkowski, A.; Pakula, M.; Biniak, A.; Bystrzejewski, M.; Szmigielski, R. Characteristic of activated carbon prepared from waste PET by carbon dioxide activation. *J. Anal. Appl. Pyrolysis* 2013, 100, 192−198.

(16) Czepirski, L.; Szczurowski, J.; Balys, M.; Ciesinska, W.; Makomaski, G.; Zielinski, J. Pore structure of activated carbons from waste polymers. *Inz. Ochr. Srodowiska* 2013, 16, 353−359.

(17) Dias, J. M.; Alvim-Ferraz, M. C. M.; Almeida, M. F.; Rivera-Utrilla, J.; Sanchez-Polo, M. Waste materials for activated carbon preparation and its use in aqueous-phase treatment: A review. *J. Environ. Manage.* 2007, 85, 833−846.

(18) Libra, J. A.; Ro, K. S.; Kammann, C.; Funke, A.; Berge, N. D.; Neubauer, Y.; Titirici, M.-M.; Fühner, C.; Bens, O.; Kern, J.; Emmerich, K.-H. Hydrothermal carbonization of biomass residuals: A comparative review of the chemistry, processes and applications of wet and dry pyrolysis. *Biofuels* 2011, 2, 89−124.

(19) Brunauer, S.; Emmett, P. H.; Teller, E. Adsorption of gases in multimolecular layers. *J. Am. Chem. Soc.* 1938, 60, 309−319.

(20) Sing, K. S. W.; Everett, D. H.; Haul, R. A. W.; Moscou, L.; Pierotti, R. A.; Roquerol, J.; Siemieniewska, T. Reporting physisorption data for gas/solid systems with special reference to the determination of surface and porosity. *Pure Appl. Chem.* 1985, 57, 603−619.

(21) Jagiello, J.; Olivier, J. P. 2D-NLDFT Adsorption models for carbon slit-shaped pores with surface energetical heterogeneity and geometrical corrugation. *Carbon* 2013, 55, 70−80.

(22) Jagiello, J.; Olivier, J. P. Carbon slit pore model incorporating surface energetical heterogeneity and geometrical corrugation. *Adsorption* 2013, 19, 777−783.

(23) Gregg, S. J.; Sing, K. S. W. *Adsorption, Surface Area and Porosity*, 2nd ed.; Academic Press: New York, 1982.

(24) Przepiorski, J.; Tryba, B.; Morawski, A. W. Adsorption of carbon dioxide on phenolic-based carbon spheres. *Appl. Surf. Sci.* 2002, 196, 296−300.

(25) Zukal, A.; Jagiello, J.; Mayerova, J.; Cejka, J. Thermodynamics of CO_2 on functionalized SBA-15 silica. NLDFT analysis of surface energetic heterogeneity. *Phys. Chem. Chem. Phys.* 2011, 13, 15468−15475.

(26) De Canck, E.; Ascoop, I.; Sayari, A.; Van Der Voort, P. Periodic mesoporous organosilicas functionalized with a wide variety of amines for CO_2 adsorption. *Phys. Chem. Chem. Phys.* 2013, 12, 9792−9799.

(27) Zhang, Z.; Zhou, J.; Xing, W.; Xue, Q.; Yan, Q.; Yan, Z.; Zhuo, S.; Qiao, S. Z. Critical role of small micropores in high CO_2 uptake. *Phys. Chem. Chem. Phys.* 2013, 15, 2523−2529.

(28) Wickramaratne, N.; Jaroniec, M. Activated carbon spheres for CO_2 adsorption. *ACS Appl. Mater. Interfaces* 2013, 5, 1849−1855.

(29) Ludwinowicz, J.; Jaroniec, M. Potassium salt-assisted synthesis of highly microporous carbon spheres for CO_2 adsorption. *Carbon* 2015, 82, 297−303.

(30) Aaron, D.; Tsouris, C. Separation of CO_2 from flue gas: A review. *Sep. Sci. Technol.* 2005, 40, 321−348.

(31) Samanta, A.; Zhao, A.; Shimizu, G. K. H.; Sarkar, P.; Gupta, R. Post-combustion CO_2 capture using solid sorbents: A review. *Ind. Eng. Chem. Res.* 2012, 51, 1438−1463.

(32) Choma, J.; Osuchowski, L.; Dziura, A.; Kwiatkowska-Wojcik, W.; Jaroniec, M. Adsorption properties of activated carbons obtained from Kevlar® fibers. *Ochr. Srodowiska* 2014, 36, 3−8.

(33) Jagiello, J.; Betz, W. Characterization of pore structure of carbon molecular sieves using DFT analysis of Ar and H_2 adsorption data. *Microporous Mesoporous Mater.* **2008**, *108*, 117−122.